

Self-Immolative Polymeric Prodrug for Targeted Cancer Therapy through Disturbing the Redox Balance

Jiyeon Kim¹, Anup Dey², Jueun Jeon², Jae-Hyung Park^{1,2,*}

¹Department of MetaBioHealth, Sungkyunkwan University, Suwon, Republic of Korea

²School of Chemical Engineering, College of Engineering, Sungkyunkwan University, Suwon, Republic of Korea

Abstract

Quinone methide (QM) is widely used in cancer therapy due to its ability to deplete glutathione (GSH), which is overexpressed in cancer cells to mitigate oxidative stress caused by high reactive oxygen species (ROS) levels. To enhance the targetability of QM, we designed a self-immolative polymeric prodrug (SIPP) with a polymer backbone and boronic ester as the terminal group. A single H_2O_2 molecule reacts with the boronic group, triggering the self-immolative degradation of the polymer and generating QM in a cascade-amplified manner. SIPP@MBE is formulated into micelles loaded with 2-methoxy- β -estradiol (MBE), which generates intracellular ROS. Upon degradation of SIPP@MBE, MBE is released and elevates the ROS levels in the tumor microenvironment, further triggering SIPP degradation. SIPP@MBE shows cytotoxicity in cancer cells while sparing normal cells. Furthermore, SIPP@MBE inhibited tumor growth in a tumor-bearing mouse model, demonstrating its potential as an effective therapeutic agent.

Result

• Characterization of SIPP@MBE

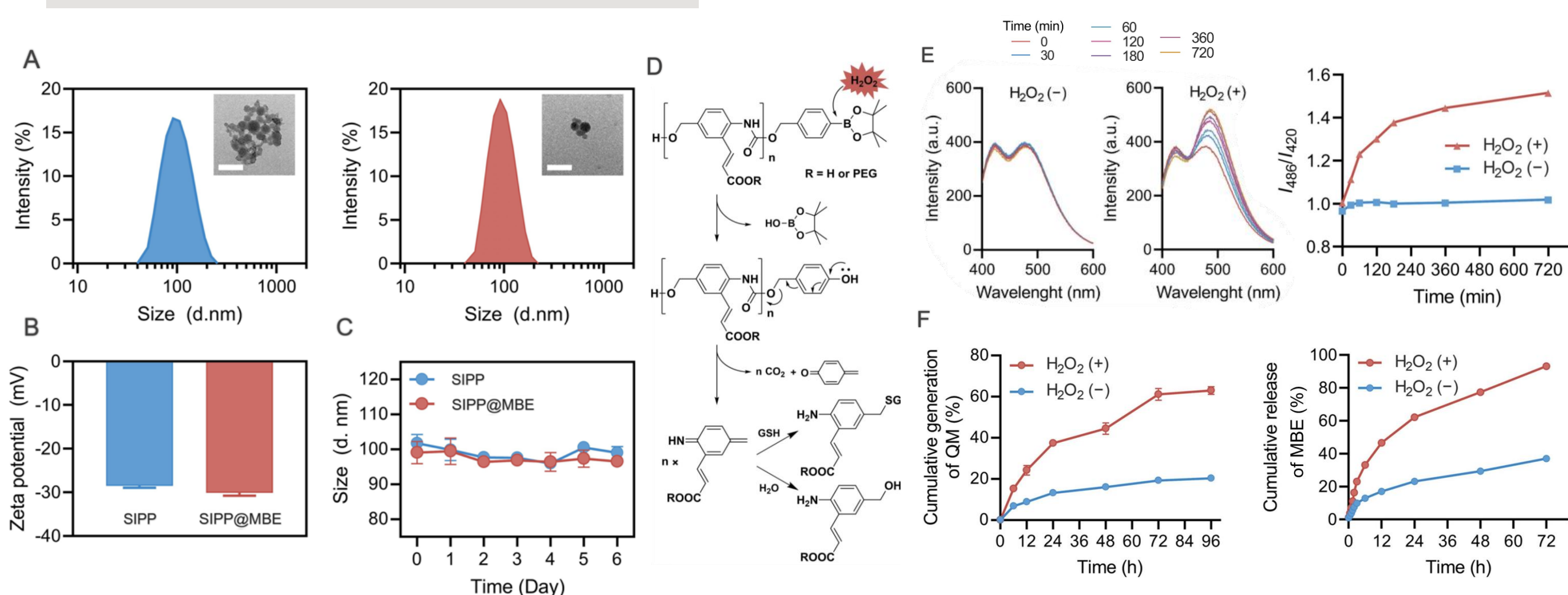


Figure 1. (A) TEM image and size distribution of SIPP (left) and SIPP@MBE (right). Scale bars: 200 μ m. (B) Zeta potential values of SIPP and SIPP@MBE. (C) Changes in the hydrodynamic size of SIPP and SIPP@MBE in PBS solution for 6 days. (D) Schematic illustration of SIPP degradation and QM generation induced by H_2O_2 . (E) Time-dependent fluorescence spectra of SIPP in DMSO in the presence of 100 μ M and absence of H_2O_2 (left) and fluorescence intensity ratio between 486 and 420 nm (right). (F) QM production (left) and MBE release (right) from SIPP@MBE in the presence and absence of H_2O_2 as a function of time. Error bars represent standard deviation (SD) ($n = 3$).

• GSH depletion by SIPP@MBE

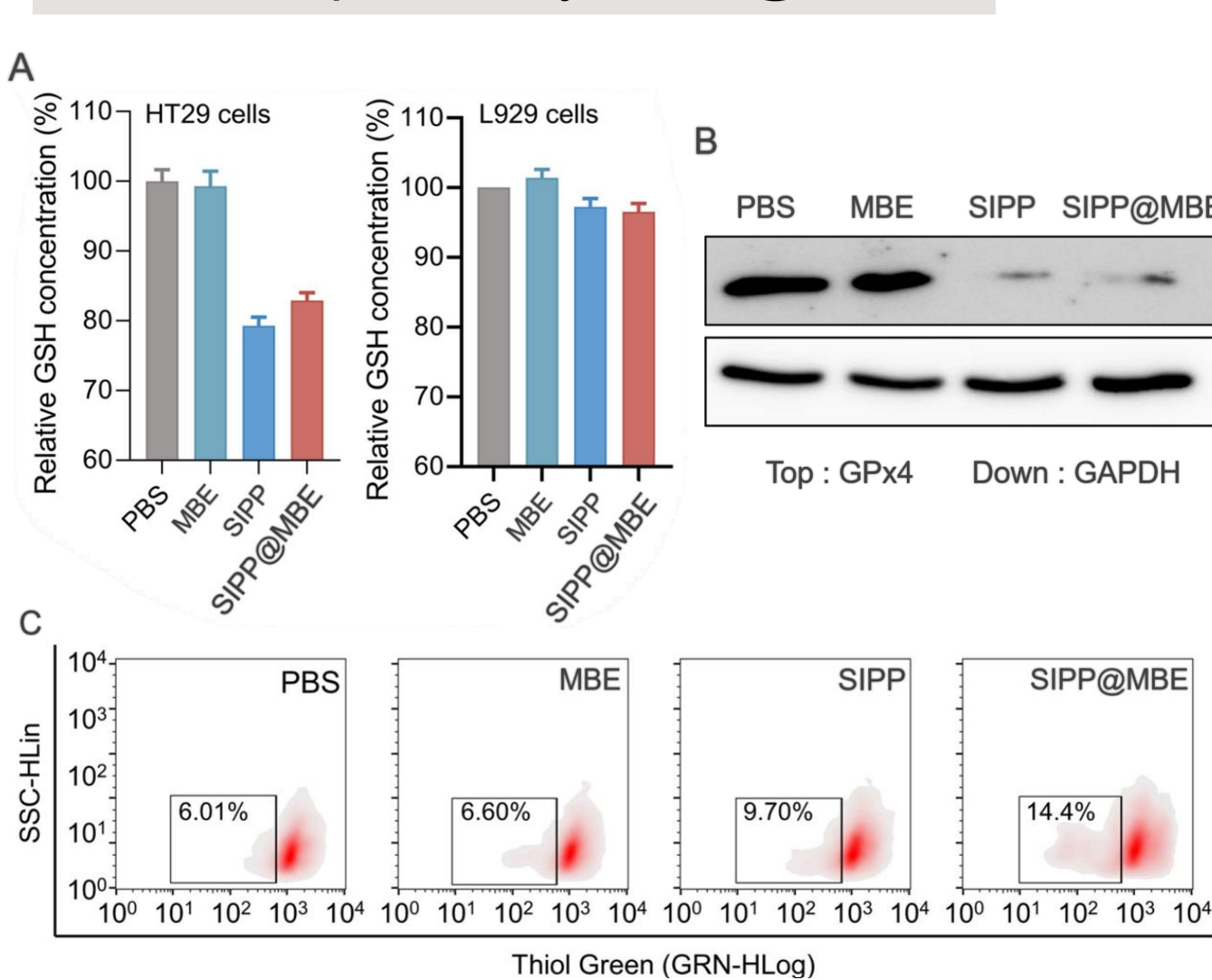


Figure 2. (A) Quantitative analysis of intracellular GSH level using Ellman's assay in HT29 cells (left) and L929 cells (right). (B) The expression level of GPx4 protein as a GSH indicator in HT29 cells. (C) Representative quantification of intracellular GSH levels in HT29 cells by flow cytometry ($n = 3$).

• Oxidative stress induced by SIPP@MBE

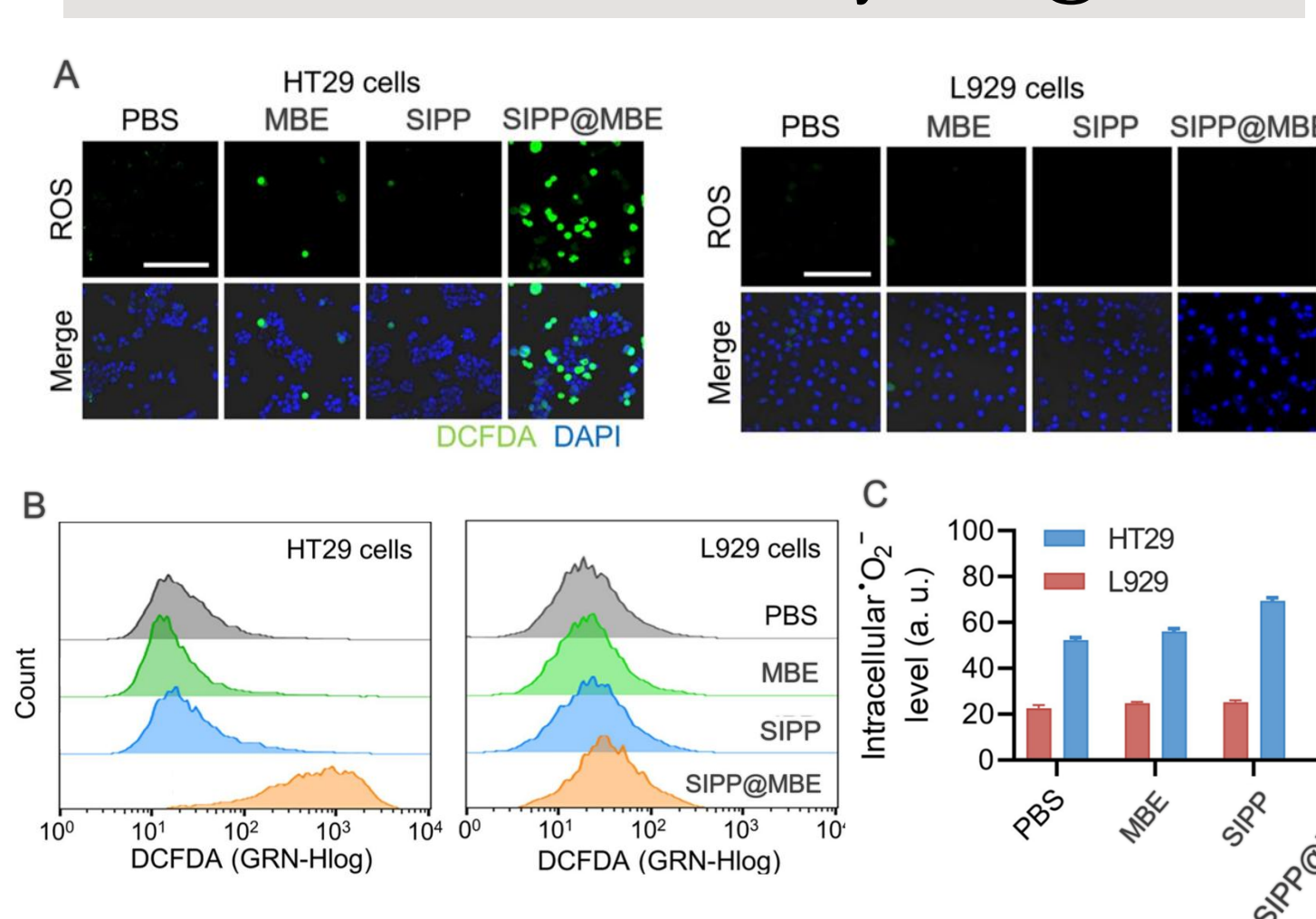


Figure 3. (A) Confocal laser microscopy images of intracellular ROS levels in HT29 cells and L929 cells. Scale bar: 30 μ m. (B) Quantitative analysis of intracellular ROS in HT29 cells and L929 cells by flow cytometry ($n = 3$). (C) Representative mean fluorescence intensity (MFI) of intracellular $O_2^{\bullet-}$ in HT29 cells measured by flow cytometry ($n = 3$).

• In vitro anticancer efficacy with SIPP@MBE

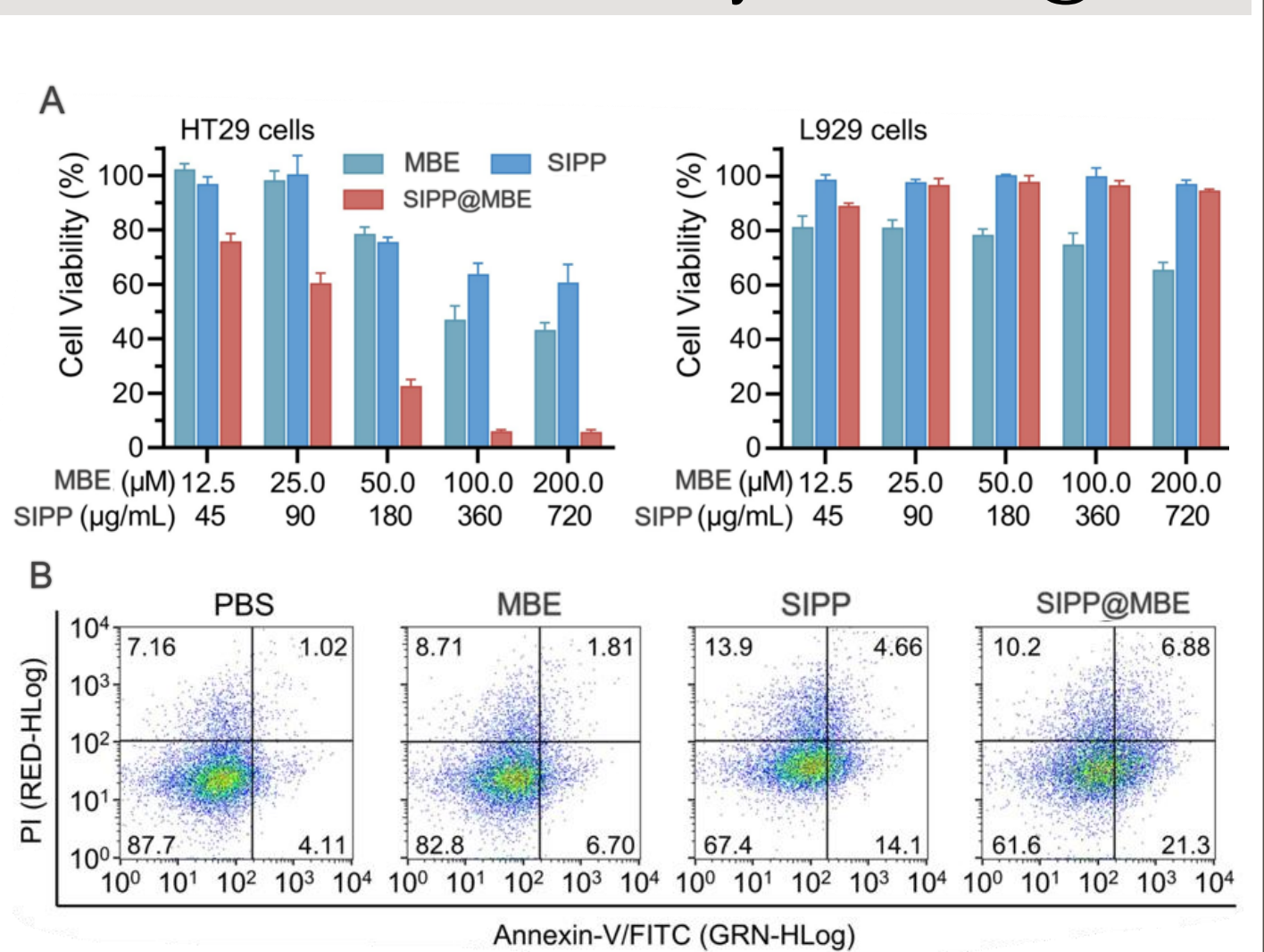


Figure 4. (A) *In vitro* cytotoxicity of MBE, SIPP, SIPP@MBE in HT29 cells and L929 cells determined by MTT. The error bars represent SD ($n = 5$). (B) Representative plots of flow cytometric analysis for annexin V/propidium iodide (PI) tests in HT29 cells.

• In vivo therapeutic efficacy with SIPP@MBE

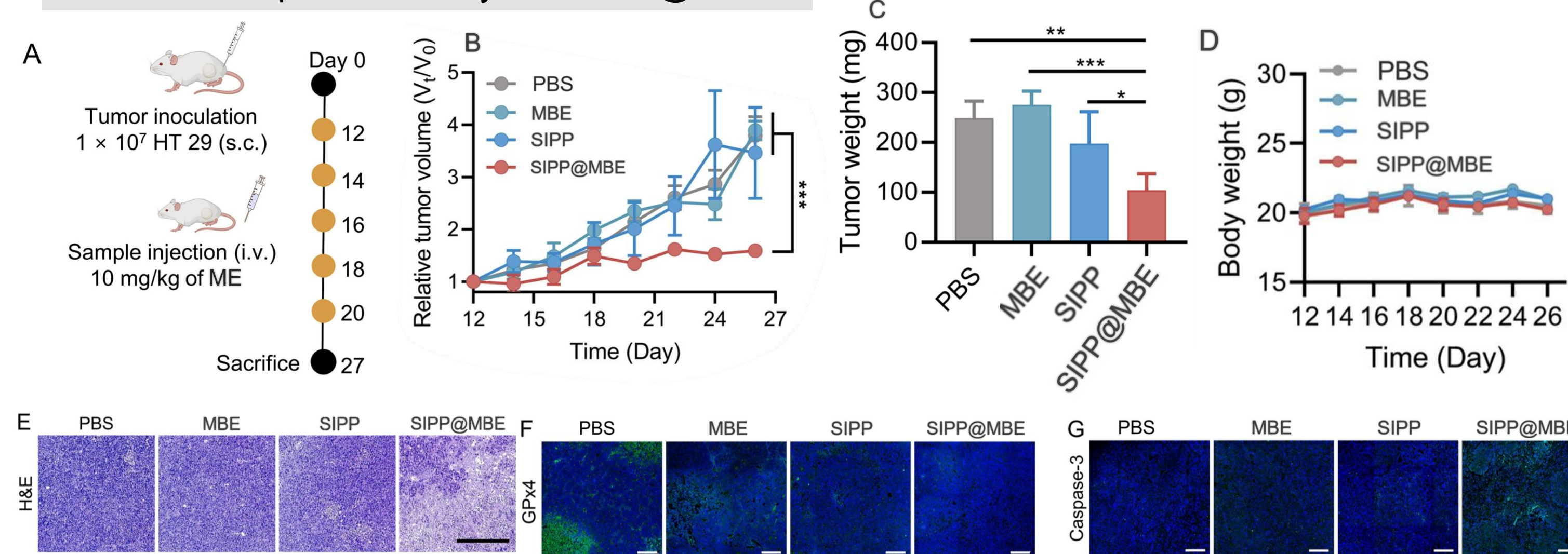


Figure 5. (A) Experimental schedule of therapy for HT29 tumor-bearing mice. (B) Tumor volumes were measured from day 12 post inoculation. (C) Weight of excised tumors. (D) Changes in body weight over time following treatment. Error bars represent the standard error of the mean (SEM) ($n = 5$). Statistical significance was analyzed by one-way ANOVA, * $p < 0.05$, ** $p < 0.01$, *** $p < 0.005$. (E) H&E staining of tumor tissues after mice were sacrificed. Immunohistochemical staining of (F) GPx4 and (G) caspase-3. Scale bar: 200 μ m.

Conclusion

SIPP@MBE was activated only in cancer cells, and its stepwise degradation released QM, scavenging GSH. As SIPP degraded, MBE was released, increasing ROS levels and disrupting the redox balance. This mechanism resulted in remarkable anticancer efficacy *in vivo*, demonstrating the potential of SIPP@MBE as an effective antitumor agent and providing insights for innovative nanomedicine development.

Reference / Acknowledgement

- [1] J. Rautio et al, Nat. Rev. Drug Discov, 2018.
- [2] I. Ekladios et al, Nat. Rev. Drug Discov, 2019.
- [3] A. Sagi et al, J. Am. Chem. Soc., 2008.
- [4] J. Jeon et al, Chem. Mater., 2022.

This work was supported by the National Research Foundation of Korea (NRF) grant funded by the Korea government (MSIT) (No. RS-2023-00256265).